Monitoring the Setting of Calcium Sulfate Bone-Graft Substitute Using Ultrasonic Backscattering

Josep Rodríguez-Sendra, Noé Jiménez, Rubén Picó, Joan Faus, and Francisco Camarena

***Abstract*— We report a method to monitor the setting process of bone-graft substitutes (calcium sulfate) using ultrasonic backscattering techniques. Analyzing the backscattered fields using a pulse-echo technique, we show that it is possible to dynamically describe the acoustic properties of the material which are linked to its setting state. Several experiments were performed to control the setting process of calcium sulfate using a 3.5-MHz transducer. The variation of the apparent integrated backscatter (AIB) with time during the setting process is analyzed and compared with measurements of the speed of sound (SOS) and temperature of the sample. The correlation of SOS and AIB allows us to clearly identify two different states of the samples, liquid and solid, in addition to the transition period. Results show that using backscattering analysis, the setting state of the material can be estimated with a threshold of 15 dB. This ultrasonic technique is indeed the first step to develop real-time monitoring systems for time-varying complex media as those present in bone regeneration for dental implantology applications.**

***Index Terms*— Bone-graft substitute, guided bone regeneration (GBR), implantology, synthetic bone substitutes, ultrasonic backscattering.**

I. Introduction

DENTAL implants require sufficient bone volume to achieve stability and durability. The loss of tooth affects the quality and thickness of the bone. In the cases where bone volume is insufficient, guided bone regeneration (GBR) techniques are applied [1]. In particular, GBR by maxillary sinus floor augmentation procedures are used since 50 years and were first proposed by Tatum: he started to use the technique in 1974 and the procedure description was published a decade after [2]. This operation, also termed sinus lift or sinus graft, is a surgical procedure which aims to increase the amount of bone in the posterior maxilla (upper jaw bone), in the area of the premolar and molar teeth. A window in the lateral area of the gingival is performed, the Schneider membrane is lifted, and a bone graft inserted. The window is coated with a pericardium membrane. The goal of the sinus augmentation is to graft extra bone into the maxillary sinus to increase the bone available to support a dental implant. Full bone regeneration process has a typical healing duration of approximately six months. The procedure sometimes fails [3] and different complications may appear postoperatively, e.g., soft tissue growth or failed osseointegration [4]. Odontologists make use of X-ray radiological techniques in order to evaluate the bone regeneration process [5]. However, monitoring the full regeneration process using these techniques implies potential risks, such as excessive exposure to ionizing radiation [5], [6]. In this sense, noninvasive ultrasonic techniques are desirable to monitor bone-regeneration during the healing time since they are non-ionizing.

Conventional ultrasonic imaging has been proposed in odontology to image tooth and asses alveolar bone structures and their morphology [7]–[10], or to detect fractured tooth, e.g., using nonlinear elastic wave spectroscopy [11]. However, these techniques do not offer quantitative indexes about the bone, as required for monitoring guided bone regeneration. On the contrary, quantitative ultrasound has been used fruitfully to characterize the physical properties of bone. Technology for bone density estimation is nowadays mature [12]–[15]. Many commercial devices exist in the market used for the diagnosis of osteoporosis, e.g., for calcaneus or phalanx [16], [17]. Acoustic and elastic parameters are correlated with the physical properties of bone for diagnostic purposes.

The speed of sound (SOS) is one of the most used parameters for quantitative ultrasound [12, Chapter 3]. It consists in estimating the effective traveling velocity of a pulsed excitation, associated with the group speed of longitudinal waves in a given frequency band. Remark that bone tissue is a heterogeneous biphasic medium composed of a multiple-scale porous viscoelastic matrix, soft-solids, and viscous fluids [12]. Therefore, acoustic propagation through these complex media is strongly dispersive and SOS, given as a single value, should be interpreted as an effective parameter rather than an intrinsic physical parameter locally related to the mechanical properties

Manuscript received March 26, 2019; accepted July 1, 2019. Date of publication July 3, 2019; date of current version September 25, 2019. This work was supported in part by Universitat Politècnica de València (UPV) and Fundación para el Fomento de la Investigación Sanitaria y Biomédica de la Comunitat Valenciana (FISABIO) through the project OSEODENT under Grant POLISABIO 2018, in part by the European Union, in part by Generalitat Valenciana through the European Regional Development Fund Program under Grant IDIFEDER/2018/022, and in part by the Agència Valenciana de la Innovació through the Unitat Científica d'Innovació Empresarial under Grant INNCON00/18/9. The work of N. Jiménez was supported by Generalitat Valenciana under Grant APOSTD/2017/042. *(Corresponding author: Josep Rodríguez-Sendra.)*

J. Rodríguez-Sendra, N. Jiménez, and F. Camarena are with the Instituto de Instrumentación para Imagen Molecular (i3M), Consejo Superior de Investigaciones Científicas (CSIC)–Universitat Politècnica de València (UPV), 46022 València, Spain (e-mail: jorodsen@upv.es).

R. Picó is with Instituto para la Gestión Integrada de Zonas Costeras (IGIC), Universitat Politècnica de València (UPV), 46730 Grau de Gandia, Spain.

J. Faus is with the Instituto Valenciano de Investigaciones Odontológicas (IVIO), 46701 Gandia, Spain.

Digital Object Identifier 10.1109/TUFFC.2019.2926827

0885-3010 © 2019 IEEE. Personal use is permitted, but republication/redistribution requires IEEE permission.
See http://www.ieee.org/publications_standards/publications/rights/index.html for more information.

of the bone. In fact, both group and phase speed in bone are a function of frequency. For example, in high mass density samples of bovine trabecular bones, the phase speed of the fast modes can vary 250 m/s in the frequency range of 0.5–3 MHz [18], while in cortical bovine bone samples it has been observed a variation of the phase speed of 20 m/s in the frequency range of 3.5–4.5 MHz [19].

In essence, SOS can be measured in pulse-echo mode using one transducer and a sample of known thickness, or in transmission mode using one emitter and one receiver transducer separated a known distance. When a single value of SOS is used to characterize the medium, a simple approach is to use the ratio between the total path traveled by the ultrasonic pulse and the total time-of-flight [20]. Other techniques include ultrasound axial transmission that has been applied to asses bone mineralization as a diagnostic technique for the evaluation of fracture healing [21]. In odontology, ultrasound transmission velocity has been proposed to evaluate bone quality before dental implantation, where they observed values of 1538 ± 177 m/s for female maxilla, 1713 ± 153 m/s for female mandible [22]. Clinical studies include the use of quantitative ultrasound to evaluate the loss of mandibular bone, where the good correlation was found between SOS values, alveolar bone density, and the attachment level around teeth in women with periodontitis [23].

Due to their complex heterogeneous microstructure, ultrasonic waves traveling in bones are microscattered in a diffuse way, as can be observed in bone-tissue simulations [24]. In this way, the interference of multiple scattered waves from internal microstructures can be received at source position offering information about the material composition. During last two decades, different techniques based on the backscatter energy evaluation have been proposed for bone characterization [25], [26]. Ultrasonic backscatter energy can be linked to the physical properties of bone tissue such as bone volume fraction or bone mineral density [12], [27], [28], enabling quantitative ultrasound techniques for bone characterization.

Many ultrasonic backscattering techniques are based on the measurements of the apparent backscatter transfer function (ABTF) [12]. It represents the backscattered power from the sample corrected for the frequency response of the measurement system. Two parameters without explicit dependence of frequency are obtained from ABTF. The apparent integrated backscatter (AIB) is one of the most spread. It consists of a measure of the frequency-averaged (integrated) backscattered power contained in some portion of a backscattered ultrasonic signal [29]. The frequency slope of apparent backscatter (FSAB) is determined by fitting a line in the frequency domain to the spatially averaged backscattered ultrasonic signals over the analysis bandwidth [30]. Both AIB and FSAB are determined in a logarithmic scale and are referenced to the measured reflected energy of a reference flat panel, e.g., a steel sample. In order to remove this reference, Hoffmeister proposed in [31] a set parameters that compare the backscatter energy from two different parts of the sample. The mean of the backscatter difference spectrum (MBD) is obtained by frequency averaging the difference between the backscatter spectra over the analysis bandwidth from two consecutive windows of the ultrasonic signal. In the context of clinical studies, other parameters, as the integrated reflection coefficient or the apparent cortical thickness, have been used to characterize the properties of bone [28], [32], [33]. In odontology, quantitative ultrasound techniques have been applied to assess the stability of dental implants [34], [35], to quantify the amount of bone in contact with dental implants [36] or to asses osseointegration of a implants *in vitro* during bone healing [37].

During the bone regeneration process, its mechanical properties are modified from the initial bone graft to the consolidated bone. A change of state is produced as a consequence of osseointegration. Thus, a solution for detecting possible anomalies during the healing of bone in GBR applications consists of monitoring the ultrasonic properties of tissue during the time. In this sense, ultrasound techniques have been applied for the characterization of slowly time-varying materials. One relevant example is cement that has been characterized by ultrasonic methods for more than 80 years, e.g., [38], [39]. In particular, pulse-echo ultrasonic techniques can be used to characterize the time dependence of SOS and the acoustic impedance during their setting process [40]–[42]. Cement starts to set when mixed with water and a series of hydration chemical reactions are produced. The constituents slowly hydrate and the mineral solidifies. In particular, the typical setting duration time for bone-graft materials based on calcium sulfate ranges from 30 to 60 min [43], [44]. Same as cement setting, the GBR is a process in which the mechanical (and acoustical) properties of the material vary with time and a change of state is produced. The advantage of using a bone-graft substitute as a phantom for monitoring GBR is that the duration of the process is reduced from six months' time of healing, to less than an hour in a controlled environment.

In this work, we propose a proof of concept to monitor the GBR by sinus augmentation using ultrasonic backscattering methods. Thus, the time-varying acoustical properties of the material under inspection are obtained using an echo-impulse technique. In particular, we use a phantom of calcium sulfate [45], [46], which has already been used for GBR in the past [47], [48]. The change of state from a viscous fluid to a porous solid during the setting mimics the GBR in a much shorter duration that can be studied under laboratory conditions. We report that ultrasonic backscatter energy can be linked to the physical properties of tissue. In GBR applications, the transmission mode using a pair of ultrasonic transducers is not allowed as a receiver transducer cannot be placed behind the area under inspection. Thus, we propose the use of a single sensor improving the accessibility of medical instrumentation for tissue characterization.

II. Methods

A. Phantom Preparation

Calcium sulfate type IV (Ventura Pinkmod) is the synthetic bone substitute used to perform the experiments. In particular, in its powder state the material is calcium sulfate hemihydrate ($CaSO_4 \cdot \frac{1}{2} H_2O$) in its α form. When the hemihydrate is mixed with water, calcium sulfate dihydrate is formed in a moderate

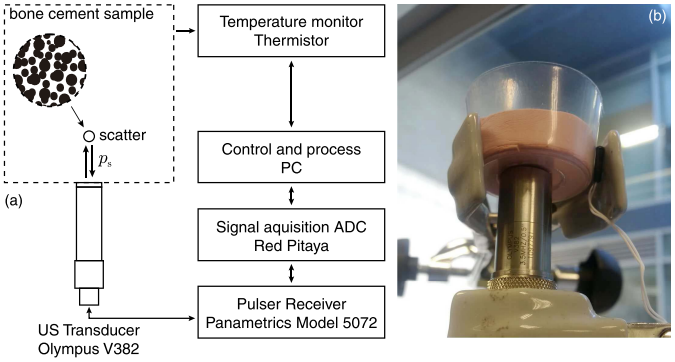


Fig. 1. (a) Block diagram of the experimental setup. (b) Photograph of one experiment.

exothermic reaction as [48]

$$\mathrm{CaSO_4 \cdot \frac{1}{2}H_2O + 1\frac{1}{2}H_2O \rightarrow CaSO_4 \cdot 2H_2O + Heat.}$$

In this way, during the setting process, the material shows a change of phase from a viscous liquid to porous solid. The total setting time is around 20 min. To study repeatability, four experiments were performed with samples composed of 23 mL of water and 50 g of calcium sulfate. The powder was dissolved in water at 20.0 ± 0.2 °C and mixed up to get homogeneous samples. The material was deposited in a cylindrical plastic container with a diameter of 36 mm to provide samples of approximately 18 mm of thickness. The thickness of the sample was measured with a Vernier caliper at different locations along the sample. The mean value was 18.3 ± 0.2 mm where the error was obtained from the standard deviation of 7 measurements.

B. Ultrasonic Measurement

An Olympus V382 transducer with a nominal central frequency of 3.5 MHz and a bandwidth of 2.34 MHz (−6 dB) was used as emitter and receiver using a pulse-echo technique. This source presents a diameter of $D = 13$ mm and a ratio between the diameter and the wavelength of $D/\lambda = 30.3$ wavelengths per aperture in water. The choice of the source is a compromise between a small physical dimension mandatory for the particular dental application and a high ratio D/λ to enhance the acoustic energy collected by the transducer. Fig. 1 shows the block diagram and a photograph of the experimental setup. The transducer was placed in contact to the bottom of the recipient in order to minimize the decoupling. Vaseline was applied between the transducer and the container and the sample to avoid decoupling during the solidification process. At the opposite side, the sample is free enhancing the reflection of the ultrasonic waves at the top interface with air. An ultrasonic pulser–receiver (Panametrics Model 5072) was used for emitting and receiving the acoustic pulses. The received signal was digitized with a data acquisition platform (Red Pitaya) at a sampling frequency of 125 MHz. For each experiment, a total of 1600 acquisitions were performed, each one every 2 s. The total duration of each experiment took 53 min, enough to cover the full setting process of the samples. The temperature was registered with thermistor probe (Tinytag Temperature Logger TK 4023) located externally in contact with the container. Measurements were postprocessed to provide the acoustic parameters during the setting process.

C. Speed of Sound

The SOS was calculated as the distance ratio between two times the thickness of the sample and the time of flight between the first two echoes from the end of the sample as

$$c = \frac{2L}{\Delta t} \tag{1}$$

where L is the thickness of the sample, and Δt is the time of flight, estimated as the times corresponding to the peak value of first two echoes. SOS was estimated during setting time, and a purely phenomenological model was fit. The proposed model describes a smooth and asymmetric transition between two phases, fluid and solid, and is given by

$$c(t) = c_1 + (c_2 - c_1)\tan^{-1}\left[\frac{\gamma}{\pi}(t - t_m) + \frac{1}{2}\right]^{\beta} \tag{2}$$

where c_1 is the SOS in liquid state, c_2 is the SOS in solid phase, γ models the speed of the transition from liquid to solid phase, t is the setting time, t_m is the half-time of the setting process, and β is related to the symmetry of the function. Remark that this simple model is purely phenomenological: it was chosen because it accurately describes the variation of the SOS during the phase transition of the samples. The fit of parameters has a physical interpretation and using them we can quantitatively compare the setting process of several experiments.

D. Backscatter Parameters

Two quantitative parameters based on the backscatter energy were considered in this work: the ABTF and the AIB energy. Both have been proven to be reliable and robust to characterize bone tissue [49]. On the one hand, the ABTF is given by the transfer function between the backscatter signal and a reference signal as

$$\mathrm{ABTF} = 10\log_{10}\left(\frac{P_s(f)}{P_{\mathrm{ref}}(f)}\right) \tag{3}$$

where $P_s(f)$ is the frequency-dependent power of a backscatter signal $p_s(t)$ using a time window of duration τ_w, and $P_{\mathrm{ref}}(f)$ is the frequency-dependent power of the first echo from a reference reflector, e.g., steel plate [49]. On the other hand, the AIB is obtained as the frequency-averaged ABTF as

$$\mathrm{AIB} = \frac{1}{\Delta f}\int_{f_1}^{f_2} \mathrm{ABTF}(f)df \tag{4}$$

where $\Delta f = f_2 - f_1$, and f_1 and f_2 are given by the −6-dB bandwidth of the transducer. The reference pulse and its spectrum are shown in Fig. 2(b) and (c), respectively. The corresponding values for the effective limiting frequencies are $f_1 = 3.4$ MHz and $f_2 = 4.6$ MHz.

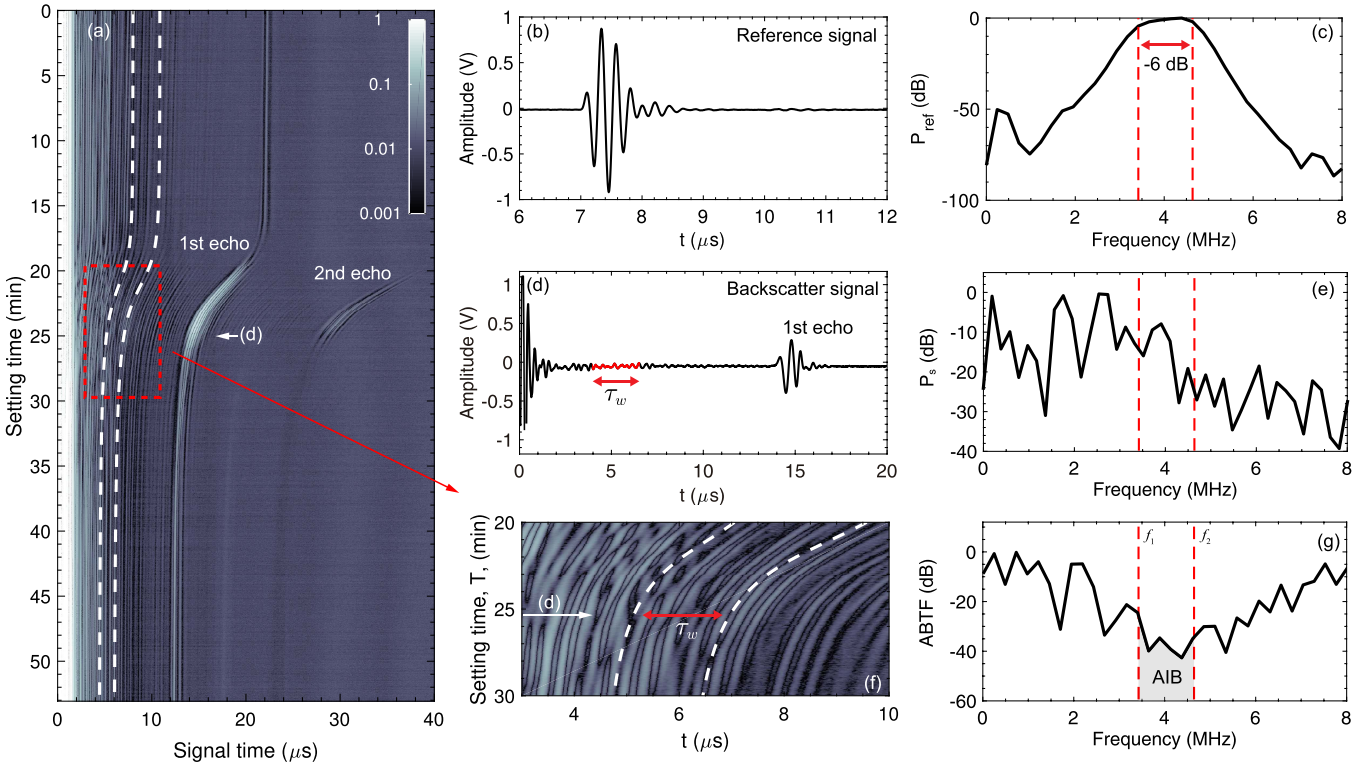


Fig. 2. (a) Representation of all the experimental signals (RAW data) as a function of the setting time. Colormap in the normalized dB scale. The white dashed lines mark the temporal window used to calculate the AIB energy. (b) Reference signal and (c) corresponding spectrum. (d) Example of a backscatter signal measured at $t = 25$ min and its (e) corresponding spectrum. (f) Zoomed in view of the experimental data over the transition period. (g) ABTF and representation of the AIB energy (shaded area).

III. Results

A. Description of Backscatter Signals

The experimental signals of one experiment are shown in Fig. 2. First, in Fig. 2(a), the A-lines are presented as a function of the setting time. Here, the amplitude of the ultrasonic signal registered by the transducer is represented in logarithmic scale normalized to the maximum value for visualization. The vertical axis represents the time of the experiment during the setting process (in minutes) and the horizontal axis represents the time of the ultrasonic signal (in μs). As both scales are very different ($\sim 10^6$), they are decoupled and each ultrasonic capture is assumed to be instantaneous.

From $t = 0$ μs to $t = 2$ μs, all ultrasonic signals have a maximum value of 0 dB corresponding to the emission pulse. Then, vertical gray traces appear corresponding to the received backscattered waves. First, when the experiment is started, the sample presents a viscous fluid state. At the beginning of the experiment time, at the top of Fig. 2(a), the echo from the end of the sample is visible at $t = 23$ μs. Up to about 15 min, the backscatter signals are stable and only small changes are visible, as shown by the straight vertical traces in the map. However, from about 18 to 27 min a sudden and drastic change in the signal is observed: the line corresponding to the echo from the back of the sample is shifted toward the beginning of the signal. This temporal compression of the signal is related to the increase of SOS in the material: the echo from the back is arriving sooner, as we will see after. Then, at 27 min, the signals become stable again and, therefore, SOS may present a stable value at the end of the experiment. At 50 min, the sample is physically a porous solid material.

Dashed lines in Fig. 2(a) show the limits for the temporal window used for the postprocessing of the backscattering. For their estimation, both the initial and final temporal values were corrected using the SOS in order to capture a constant spatial window. Fig. 2(f) shows in detail the tracking of lines during the transition from the liquid state to solid state in the setting process. Here, the traces of the captured backscattered waves match the analysis window marked by the dashed white lines.

Backscatter parameters have been referenced to a signal obtained from a flat steel plate, shown in Fig. 2(b). An example of A-scan signal registered by the transducer using the bone-graft substitute sample (at $t = 25$ min) is shown in Fig. 2(d). Both the initial electrical contribution and the first echo caused at the end of the sample can be observed at $t = 0$ μs and $t = 15$ μs, respectively. In comparison, backscattered energy is very low and spreads all along the signal. We consider a window of the duration of $\tau_w = 2.8$ μs, i.e., 10 times the period corresponding of the central frequency of the transducer at the beginning of the experiment, according to [29]. The window was set initially centered at 8 μs. Note that this value is shifted at 25 min [Fig. 2(d)] to 5 μs due to the change of SOS with the setting time [see white dashed lines in Fig. 2(a)]. The spectra of the reference signal and the example backscattered signal are shown in Fig. 2(c) and (e), respectively. Then, for each temporal

TABLE I
FIT PARAMETERS FOR THE PHENOMENOLOGICAL MODEL GIVEN BY (2)

	Transition asymmetry β	Transition speed γ (min^{-1})	Transition time t_m (min)	Initial state SOS c_1 (m/s)	Final state SOS c_2 (m/s)
Sample 1 (E1)	2.1	0.346	20.7	1477.2	2731.5
Sample 2 (E2)	1.9	0.341	20.8	1399.7	2490.9
Sample 3 (E3)	1.4	0.327	19.9	1553.9	2919.5
Sample 4 (E4)	1.7	0.367	20.1	1627.2	3049.8
Mean	1.8 ± 0.3	0.345 ± 0.016	20.4 ± 0.4	1514 ± 98	2858.1 ± 155.5

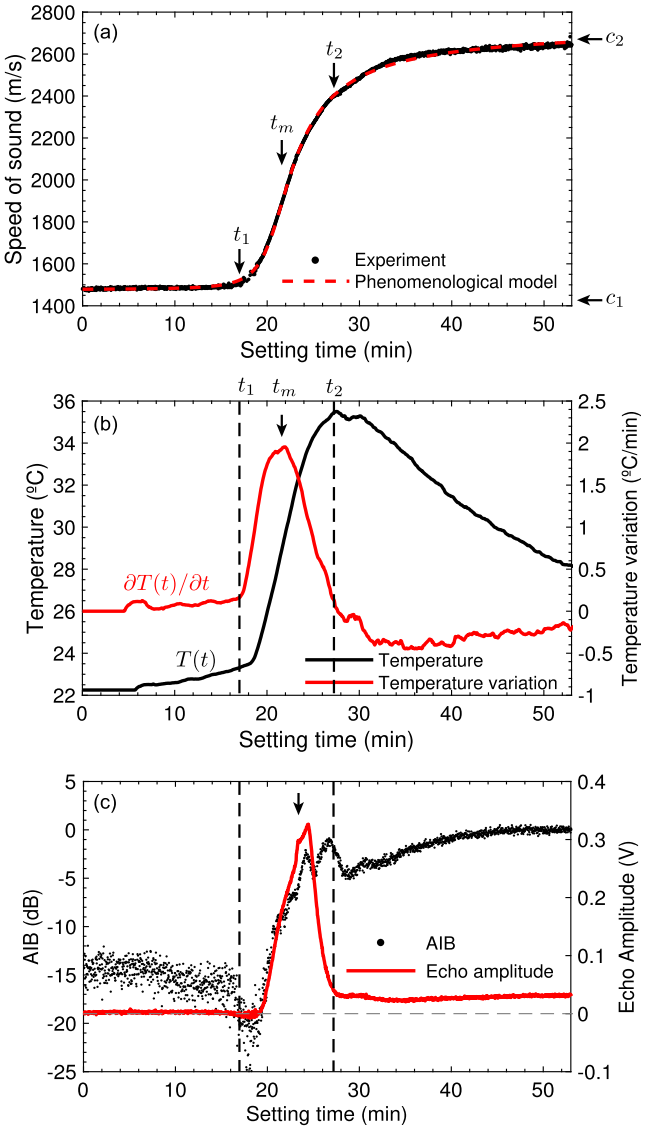


Fig. 3. (a) Evolution of the SOS, experiment (dots), and fit model (red dashed) using (2). (b) Evolution of the temperature (black) and temperature variation (red). (c) AIB energy (dots) and peak amplitude of the first echo (red), as a function of the setting time.

signal ABTF is calculated using (3), as shown in Fig. 2(f). Finally, AIB is estimated using (4) by averaging ABTF over the interest bandwidth, shown in Fig. 2(f) as the shaded region.

B. Evolution of Speed of Sound

The evolution of the SOS with the setting time is shown in Fig. 3(a). In addition, the evolution of the temperature and its variation, i.e., $\partial T/\partial t$, are shown in Fig. 3(b). The initial value measured for the SOS corresponds to $c_1 = 1477 \pm 50$ m/s close to the value of liquid water at same temperature (1495 m/s). The value estimated for the error is the standard deviation of seven consecutive pulse-echo measurements. Up to $t_1 = 17.32$ min, temperature is approximately stable and its rate of variation is small, about 0.1 °C/min. However, after this time (t_1), the chemical reaction between the calcium sulfate and water suddenly increases. When the temperature starts to increase small variations of SOS were already detected.

The maximum temperature variation is achieved at 21.6 min, corresponding to 1.9 °C/min. This point corresponds to the maximum exothermic chemical activation [50]. Note this time almost corresponds to the time $t_m = 20.7$ min given by the SOS model fit. After that moment, there is more consolidated material than calcium sulfate hemihydrate and water available to maintain the chemical reaction at this rate and, therefore, the exothermic activity is smoothly reduced. Then, at $t_2 = 27.6$ min the temperature reaches its maximum value, 35.5 °C. The sample starts to cool smoothly due to heat diffusion processes and the lack of chemical activity. Once the change of state is completed, the sample is transformed from a viscous liquid to porous solid material. When the material is solidified, the SOS reaches a stable value close to $c_2 = 2731.5$ m/s. The behavior of this synthetic bone substitute agrees the one reported for other cements measured using an emission/reception mode [40]–[42].

As expected, it can be observed that the change of the state of the material corresponds to an abrupt increase of the SOS. This particular smooth transition was measured in all samples and can be described by three different phases: the liquid state, the transition, and the solid state. The experimental SOS data were fit to the phenomenological model given by (2). The parameters of the fit model describe quantitatively the setting process. These parameters are listed in Table I for the four samples, showing similar values between experiments.

First, the parameter c_1 is linked to the physical SOS at the initial viscous-liquid state of the sample. The mean value of c_1 over the four experiments is 1514 ± 98 m/s. As the material at the initial process is mainly water with the undissolved powder, the SOS measured for the sample is close to the SOS of the water. The final value of the SOS in the experiment is related to c_2, i.e., the SOS of the material in the solid state. The mean value of c_2 is 2858 ± 155 m/s.

The transition time for the setting process is given by the parameter t_m. This parameter takes a mean value of $t_m = 20.4$ min, very close to the peak of maximum exothermic chemical activity (21.6 min for sample 1). The factor γ is related to the duration of the transition from liquid to solid

state, its mean value is $1.8 \pm 0.3\ \text{min}^{-1}$. Finally, the factor β is related to the symmetry of the function and takes a mean value of 0.345 ± 0.016. The dispersion of the parameters is low, and all experiments present similar transition curves. However, some discrepancies are observed in SOS values, that can be associated with uncertainness on estimating the thickness of the sample L.

C. Evolution of Apparent Integrated Backscatter Energy

In addition to SOS, energetic parameters also can provide information about the change of phase of calcium sulfate. In particular, we show in Fig. 3(c) the AIB as a function of the setting time. Moreover, the amplitude of the 1st echo is also shown by the red curve in Fig. 3(c). When the sample is in a viscous-liquid state, from $t = 0$ to about t_1, the mean value of AIB is low and constant, taking a value of about -15 dB. However, the AIB estimations present high dispersion due to the low amplitude of the backscatter signals. Note that, in addition, the amplitude of the 1st echo is also very low. The weak scattering and the weak echo reflection are caused by the strong absorption and high homogeneity of the sample in its initial viscous-liquid phase. When the exothermic chemical reaction starts, both AIB and echo signal initially decrease. AIB takes a value down to -20 dB at 20 min.

However, as the reaction continues (after t_1) both the scattering energy and the peak amplitude of the echo increase: the intrinsic absorption of the consolidated synthetic bone substitute is lower compared to its viscous-fluid phase. Thus, AIB progressively increases and its dispersion is reduced. During this time, the transition of state in the setting process is produced; the mechanical and acoustic features of the sample are drastically modified and the microstructure of the porous solid material starts to consolidate, leading to an increase of the amplitude of the backscatter signal. The consolidated material presents less absorption, and at the middle of the transition. the echo from the back arrives with remarkable amplitude. However, as the porous solid consolidates its inner microstructure the backscatter energy increases. As a consequence, the amplitude of the first echo of the back is again reduced as waves reach the end of the sample with a lower amplitude. After some small oscillations during the transition, the AIB ends with a value of about -5 dB at 25 min.

Finally, after 30 min, the sample is transformed to solid state and the AIB is smoothly increased from -5 dB to a plateau reaching a maximum value 0 dB at 50 min. Therefore, while the dispersion of the AIB is low and it reaches a stable value, the amount of the energy of the ultrasonic pulse that reaches the end of the sample is reduced due to scattering processes. This is caused by the final properties of the bone-graft substitute that present high microheterogeneity and porosity. After this time, the setting process is completed and the material is mechanically and acoustically stable.

D. Correlation Between SOS and AIB

While at the initial and the end of the setting time AIB takes different values, AIB presents some oscillations during the setting period. These can lead to uncertainness if used to monitor the setting of the material. A deeper analysis can be performed by showing the correlation between AIB and SOS. Fig. 4(a)–(d) shows this correlation for the four experiments. For each experiment, the insets show the corresponding histograms for SOS and AIB data, where two peaks corresponding to the initial and final states can be observed.

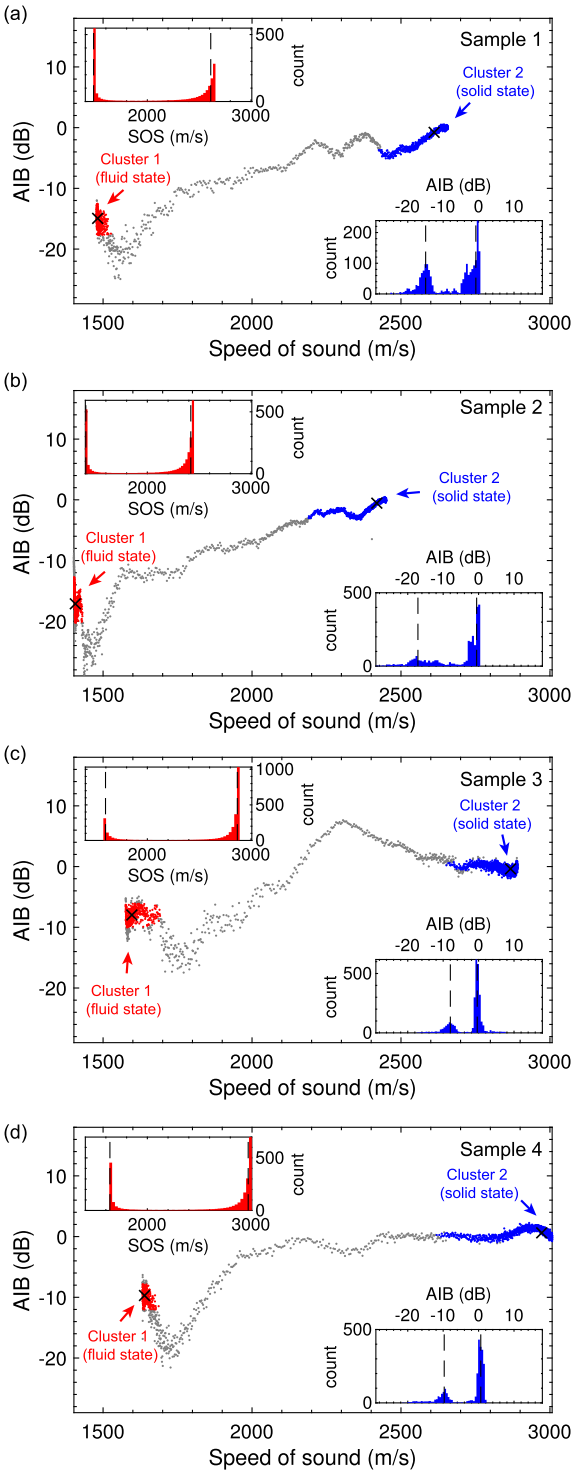


Fig. 4. (a)–(d) Correlation of AIB and SOS and clustering for the four samples. Insets: corresponding histograms of the SOS (red) and AIB (blue). Each detected cluster is shown in red and blue, corresponding to a different state. The mean value of each cluster is marked by black crosses.

While there exists a positive correlation between AIB and SOS, the data show some oscillations.

A concentration of experimental points can be observed in two zones, marked by arrows. On the one hand, when the material is in its viscous liquid phase is when the values of SOS are minimum. On the other hand, when the material is a porous solid both SOS and AIB present maximum values. As experimental data concentrates in these two limits, we can apply clustering techniques to identify them. A density-based spatial clustering of applications with noise (DBSCAN) technique [51] was employed here to discern between the data corresponding to the two concentration points and the transition. This gives us the corresponding clusters marked in red and blue in Fig. 4(a)–(d), helping to monitor the setting process: when a cluster is clearly populated, the sample has reached a stable phase. Note that using only the histogram for the AIB some of the signals corresponding to the transition point can present the same AIB than in the final state due to the oscillations of this parameter, e.g., Fig. 4(c).

IV. Conclusion

The change of state of a bone-graft substitute (calcium sulfate) has been monitored and characterized by ultrasonic backscattering analysis. Temperature, SOS, and AIB energy were measured during the setting process of the sample using a pulse-echo technique. The evolution of SOS shows a smooth transition between two limiting values, corresponding to the viscous-fluid and porous solid state of the calcium sulfate samples. An excellent agreement is found between the evolution of the SOS and a simple phenomenological model to describe the setting process. The experiments also show good repeatability.

In addition, the evolution of AIB is shown to be correlated with SOS. The AIB energy is proven to be an appropriate parameter to describe the transition from a viscous-liquid state, with values around -15 dB, to a complex porous solid, with values around 0 dB. The technique based on acoustic scattering measurements of AIB is proven more robust that the SOS technique in which the imprecise measurement of the sample thickness is required.

In addition, the evolution of AIB is shown to be correlated with SOS. The AIB energy is proven to be an appropriate parameter to describe the transition from a viscous-liquid state, with values around -15 dB, to a complex porous solid, with values around 0 dB. While all experiments showed similar dynamics, in the case of the SOS differences in the initial and final values are notable. This might be caused by the uncertainties in the estimation of the thickness of the sample in the viscous-liquid phase of the bone-cement. For the AIB, there exist also discrepancies between samples, but in all the cases, the magnitude of the parameter at the final state is at least 10 dB higher than at the beginning of the experiment, and this parameter is remarkably constant at the end of the experiment. The technique based on energetic backscattering is proven more robust that ultrasonic velocity technique. Remark that for the parameter used, i.e., AIB, the measurement of the thickness is not required. This relation confirms that the backscattering analysis with ultrasound is a powerful tool to monitor complex materials with time-varying mechanical properties using an appropriate single transducer and pulse-echo techniques.

This study represents a contribution to the use of ultrasound for the monitoring of GBR, which is necessary for the successful placement of dental implants. A synthetic bone substitute has been used as a bone phantom because its mechanical properties change during the setting process from a viscous liquid to a rigid porous material, as, under reasonable simplifications, occurs in GBR applications. The technique using an appropriate single transducer might provide a low-cost system, but indeed it presents some limitations. In a clinical scenario, it will be difficult to locate the ultrasonic probe in the same point during the six-months monitoring process. Possible mitigations to this limitation can be the use of a portable low-cost phased array system to incorporate in the backscattering analysis the spatial information or the use of patient-specific dental splint to control the location of a single-element ultrasonic transducer. Therefore, many practical questions remain open and should be explored. These include the effect of the varying coupling of the transducer and the tissue between acquisitions, the mechanical/acoustical behavior of real tissue during bone regeneration, the scattering properties of these unconsolidated and consolidated tissues, patient variability, or the impact of the intrinsic properties of real bones during regeneration, e.g., porosity, viscosity, in the estimated parameters. These issues should be explored in future studies. The technique proposed here for dental implants may be also explored to survey other implant sites like the femoral neck. Of course, an appropriate transducer must be used in order to fit with the requirements for the sound field imposed by the penetration depth from the surface to the zone of inspection.

Finally, it is worth to mention that one advantage of backscattering analysis with respect to SOS is that using backscattering techniques it is not needed to know the thickness of the sample. Note using an appropriate single transducer the estimation of the thickness of the sample is critical to accurately estimate SOS and, therefore, scattering techniques might be preferred. This is a significant benefit to envisaged implant applications *in vivo* where the GBR can be monitored.

Acknowledgment

This work has been developed within the framework of the IVIO-UPV Chair of the research project of the Universitat Politècnica de València “Desarrollo de tecnologías aplicadas al campo de la odontología” and is the result of the collaboration of researchers from the Universitat Politècnica de València and the Instituto Valenciano de Investigaciones Odontológicas (IVIO) in the field of dental implantology with ultrasonic technology.

References

[1] F. Bodic, L. Hamel, E. Lerouxel, M. F. Baslé, and D. Chappard, “Bone loss and teeth,” *Joint Bone Spine*, vol. 72, no. 3, pp. 215–221, May 2005.

[2] H. Tatum, “Maxillary and sinus implant reconstructions,” *Dental Clinics North Amer.*, vol. 30, no. 2, pp. 207–229, Apr. 1986.

[3] S. Annibali, M. Ripari, G. La Monaca, F. Tonoli, and M. P. Cristalli, "Local complications in dental implant surgery: Prevention and treatment," *ORAL Implantol.*, vol. 1, no. 1, pp. 21–33, Apr./Jun. 2008.

[4] J. Acero, "Maxillary sinus grafting for implant insertion," in *Preprosthetic Maxillofacial Surgery*. Amsterdam, The Netherlands: Elsevier, 2011, pp. 54–75.

[5] A. Memon, S. Godward, D. Williams, I. Siddique, and K. Al-Saleh, "Dental X-rays and the risk of thyroid cancer: A case-control study," *Acta Oncologica*, vol. 49, no. 4, pp. 447–453, Apr. 2010.

[6] J. B. Ludlow, L. E. Davies-Ludlow, and S. C. White, "Patient risk related to common dental radiographic examinations: The impact of 2007 international commission on radiological protection recommendations regarding dose calculation," *J. Amer. Dental Assoc.*, vol. 139, no. 9, pp. 1237–1243, Sep. 2008.

[7] F. I. Tsiolis, I. G. Needleman, and G. S. Griffiths, "Periodontal ultrasonography," *J. Clin. Periodontology*, vol. 30, no. 10, pp. 849–854, Oct. 2003.

[8] S. R. Ghorayeb, C. A. Bertoncini, and M. K. Hinders, "Ultrasonography in dentistry," *IEEE Trans. Ultrason., Ferroelectr., Freq. Control*, vol. 55, no. 6, pp. 1256–1266, Jun. 2008.

[9] D. Hughes *et al.*, "Investigation of dental samples using a 35 MHz focussed ultrasound piezocomposite transducer," *Ultrason.*, vol. 49, no. 2, pp. 212–218, Feb. 2009.

[10] J. Marotti *et al.*, "Recent advances of ultrasound imaging in dentistry—A review of the literature," *Oral Surg., Oral Med., Oral Pathol. Oral Radiol.*, vol. 115, no. 6, pp. 819–832, Jun. 2013.

[11] S. Dos Santos and Z. Prevorovsky, "Imaging of human tooth using ultrasound based chirp-coded nonlinear time reversal acoustics," *Ultrasonics*, vol. 51, no. 6, pp. 667–674, Apr. 2011.

[12] P. Laugier and G. Haïat, *Bone Quantitative Ultrasound*. Berlin, Germany: Springer, 2011, vol. 576.

[13] M. L. Frost, G. M. Blake, and I. Fogelman, "Quantitative ultrasound and bone mineral density are equally strongly associated with risk factors for osteoporosis," *J. Bone Mineral Res.*, vol. 16, no. 2, pp. 406–416, Feb. 2001.

[14] K. Raum, Q. Grimal, P. Varga, R. Barkmann, C. C. Glüer, and P. Laugier, "Ultrasound to assess bone quality," *Current Osteoporosis Rep.*, vol. 12, no. 2, pp. 154–162, Jun. 2014.

[15] D. Hans and S. Baim, "Quantitative ultrasound (QUS) in the management of osteoporosis and assessment of fracture risk," *J. Clin. Densitometry*, vol. 20, no. 3, pp. 322–333, Jul. 2017.

[16] C. M. Langton, S. B. Palmer, and R. W. Porter, "The measurement of broadband ultrasonic attenuation in cancellous bone," *Eng. Med.*, vol. 13, no. 2, pp. 89–91, Apr. 1984.

[17] C. M. Langton and C. F. Njeh, "The measurement of broadband ultrasonic attenuation in cancellous bone—A review of the science and technology," *IEEE Trans. Ultrason., Ferroelectr., Freq. Control*, vol. 55, no. 7, pp. 1546–1554, Jul. 2008.

[18] K. R. Waters and B. K. Hoffmeister, "Kramers-Kronig analysis of attenuation and dispersion in trabecular bone," *J. Acoust. Soc. Amer.*, vol. 118, no. 6, pp. 3912–3920, Dec. 2005.

[19] G. Haïat, M. Sasso, S. Naili, and M. Matsukawa, "Ultrasonic velocity dispersion in bovine cortical bone: An experimental study," *J. Acoust. Soc. Amer.*, vol. 124, no. 3, pp. 1811–1821, Sep. 2008.

[20] P. H. F. Nicholson, G. Lowet, C. M. Langton, J. Dequeker, and G. Van der Perre, "A comparison of time-domain and frequency-domain approaches to ultrasonic velocity measurement in trabecular bone," *Phys. Med. Biol.*, vol. 41, no. 11, p. 2421, Nov. 1996.

[21] C. B. Machado, W. C. de A. Pereira, M. Granke, M. Talmant, F. Padilla, and P. Laugier, "Experimental and simulation results on the effect of cortical bone mineralization in ultrasound axial transmission measurements: A model for fracture healing ultrasound monitoring," *Bone*, vol. 48, no. 5, pp. 1202–1209, May 2011.

[22] M. Klein, K. Grötz, B. Manefeld, P. H. Kann, and B. Al-Nawas, "Ultrasound transmission velocity for noninvasive evaluation of jaw bone quality *in vivo* before dental implantation," *Ultrasound Med. Biol.*, vol. 34, no. 12, pp. 1966–1971, Dec. 2008.

[23] Y. Takaishi *et al.*, "Correlations between periodontitis and loss of mandibular bone in relation to systemic bone changes in postmenopausal Japanese women," *Osteoporosis Int.*, vol. 16, no. 12, pp. 1875–1882, Dec. 2005.

[24] J. J. Kaufman, G. Luo, and R. S. Siffert, "Ultrasound simulation in bone," *IEEE Trans. Ultrason., Ferroelectr., Freq. Control*, vol. 55, no. 6, pp. 1205–1218, Jun. 2008.

[25] K. A. Wear and B. S. Garra, "Assessment of bone density using ultrasonic backscatter," *Ultrasound Med. Biol.*, vol. 24, no. 5, pp. 689–695, Jun. 1998.

[26] S. Chaffaí, F. Peyrin, S. Nuzzo, R. Porcher, G. Berger, and P. Laugier, "Ultrasonic characterization of human cancellous bone using transmission and backscatter measurements: Relationships to density and microstructure," *Bone*, vol. 30, no. 1, pp. 229–237, Jan. 2002.

[27] F. Padilla, F. Jenson, V. Bousson, F. Peyrin, and P. Laugier, "Relationships of trabecular bone structure with quantitative ultrasound parameters: *In vitro* study on human proximal femur using transmission and backscatter measurements," *Bone*, vol. 42, no. 6, pp. 1193–1202, Jun. 2008.

[28] J. P. Karjalainen, J. Töyräs, O. Riekkinen, M. Hakulinen, and J. S. Jurvelin, "Ultrasound backscatter imaging provides frequency-dependent information on structure, composition and mechanical properties of human trabecular bone," *Ultrasound Med. Biol.*, vol. 35, no. 8, pp. 1376–1384, Aug. 2009.

[29] B. K. Hoffmeister, C. Jones III, G. Caldwell, and S. C. Kaste, "Ultrasonic characterization of cancellous bone using apparent integrated backscatter," *Phys. Med. Biol.*, vol. 51, no. 11, p. 2715, May 2006.

[30] B. K. Hoffmeister, A. P. Holt, and S. C. Kaste, "Effect of the cortex on ultrasonic backscatter measurements of cancellous bone," *Phys. Med. Biol.*, vol. 56, no. 19, p. 6243, Sep. 2011.

[31] B. K. Hoffmeister, A. R. Wilson, M. J. Gilbert, and M. E. Sellers, "A backscatter difference technique for ultrasonic bone assessment," *J. Acoust. Soc. Amer.*, vol. 132, no. 6, pp. 4069–4076, Dec. 2012.

[32] J. P. Karjalainen, O. Riekkinen, J. Töyräs, M. Hakulinen, H. Kröger, T. Rikkonen, K. Salovaara, and J. S. Jurvelin, "Multi-site bone ultrasound measurements in elderly women with and without previous hip fractures," *Osteoporosis Int.*, vol. 23, no. 4, pp. 1287–1295, Apr. 2012.

[33] J. T. Schousboe, O. Riekkinen, and J. Karjalainen, "Prediction of hip osteoporosis by DXA using a novel pulse-echo ultrasound device," *Osteoporosis Int.*, vol. 28, no. 1, pp. 85–93, Jan. 2017.

[34] V. Mathieu *et al.*, "Biomechanical determinants of the stability of dental implants: Influence of the bone–implant interface properties," *J. Biomech.*, vol. 47, no. 1, pp. 3–13, Jan. 2014.

[35] R. Vayron, E. Soffer, F. Anagnostou, and G. Haïat, "Ultrasonic evaluation of dental implant osseointegration," *J. Biomech.*, vol. 47, no. 14, pp. 3562–3568, Nov. 2014.

[36] V. Mathieu, F. Anagnostou, E. Soffer, and G. Haïat, "Ultrasonic evaluation of dental implant biomechanical stability: An *in vitro* study," *Ultrasound Med. Biol.*, vol. 37, no. 2, pp. 262–270, Feb. 2011.

[37] V. Mathieu, R. Vayron, E. Soffer, F. Anagnostou, and G. Haïat, "Influence of healing time on the ultrasonic response of the bone-implant interface," *Ultrasound Med. Biol.*, vol. 38, no. 4, pp. 611–618, Apr. 2012.

[38] T. R. Naik, V. M. Malhotra, and J. S. Popovics, "The ultrasonic pulse velocity method," in *Handbook on Nondestructive Testing of Concrete*. Boca Raton, FL, USA: CRC Press, 2003, pp. 182–200.

[39] T. P. Philippidis and D. G. Aggelis, "Experimental study of wave dispersion and attenuation in concrete," *Ultrasonics*, vol. 43, no. 7, pp. 584–595, Jun. 2005.

[40] J. Keating, D. J. Hannant, and A. P. Hibbert, "Comparison of shear modulus and pulse velocity techniques to measure the build-up of structure in fresh cement pastes used in oil well cementing," *Cement Concrete Res.*, vol. 19, no. 4, pp. 554–566, Jul. 1989.

[41] C. M. Sayers and R. L. Grenfell, "Ultrasonic propagation through hydrating cements," *Ultrasonics*, vol. 31, no. 3, pp. 147–153, May 1993.

[42] A. Boumiz, C. Vernet, and F. C. Tenoudji, "Mechanical properties of cement pastes and mortars at early ages: Evolution with time and degree of hydration," *Adv. Cement Based Mater.*, vol. 3, nos. 3–4, pp. 94–106, Apr./May 1996.

[43] J. Carlson, M. Nilsson, E. Fernández, and J. A. Planell, "An ultrasonic pulse-echo technique for monitoring the setting of $CaSO_4$-based bone cement," *Biomaterials*, vol. 24, no. 1, pp. 71–77, Jan. 2003.

[44] M. D. Vlad, L. González, S. Gómez, J. López, J. E. Carlson, and E. Fernández, "Ultrasound monitoring of the setting of calcium-based bone cements," *J. Mater. Sci., Mater. Med.*, vol. 23, no. 7, pp. 1563–1568, Jul. 2012.

[45] C. G. Finkemeier, "Bone-grafting and bone-graft substitutes," *J. Bone Joint Surg.*, vol. 84, no. 3, pp. 454–464, Mar. 2002.

[46] W. Wang and K. W. K. Yeung, "Bone grafts and biomaterials substitutes for bone defect repair: A review," *Bioactive Mater.*, vol. 2, no. 4, pp. 224–247, Dec. 2017.

[47] D. De Leonardis and G. E. Pecora, "Prospective study on the augmentation of the maxillary sinus with calcium sulfate: Histological results," *J. Periodontol.*, vol. 71, no. 6, pp. 940–947, Jun. 2000.

[48] M. V. Thomas and D. A. Puleo, "Calcium sulfate: Properties and clinical applications," *J. Biomed. Mater. Res. B, Appl. Biomater, Off. J. Soc. Biomater., Jpn. Soc. Biomater., Austral. Soc. Biomater. Korean Soc. Biomater.*, vol. 88, no. 2, pp. 597–610, Feb. 2009.
[49] B. K. Hoffmeister, J. A. McPherson, M. R. Smathers, P. L. Spinolo, and M. E. Sellers, "Ultrasonic backscatter from cancellous bone: The apparent backscatter transfer function," *IEEE Trans. Ultrason., Ferroelectr., Freq. Control*, vol. 62, no. 12, pp. 2115–2125, Dec. 2015.
[50] C. Liu, W. Gai, S. Pan, and Z. Liu, "The exothermal behavior in the hydration process of calcium phosphate cement," *Biomaterials*, vol. 24, no. 18, pp. 2995–3003, Aug. 2003.
[51] M. Ester, H.-P. Kriegel, J. Sander, and X. Xu, "A density-based algorithm for discovering clusters in large spatial databases with noise," in *Proc. KDD*, vol. 96, 1996, pp. 226–231.



Josep Rodríguez-Sendra received the B.Sc. degree in telecommunication and the M.Sc. degree in acoustics from the Universitat Politècnica de València (UPV) in 2014 and 2015, respectively, where he is currently pursuing the Ph.D. degree with the Instituto de Instrumentación para Imagen Molecular (i3M).

In 2016, he enrolled in the team Ultrasound Medical and Industrial Laboratory (UMIL) , València, Spain, at i3M to conduct research on ultrasonic technology applied to odontology. His research interest concerns new technologies for biomedical ultrasound applications.



Noé Jiménez received the B.Sc. degree in telecommunication, and the M.Sc. and Ph.D. degrees in acoustics from the Universitat Politècnica de València (UPV), València, Spain, in 2015.

In 2014, under funding of the European Space Agency, he worked at UPV for noise control at the launch pad using periodic structures. In 2015, he joined the Centre National de la Recherche Scientifique (CNRS UMR 6613), Le Mans, France, for a Posdoctoral Position to conduct research on deep-subwavelength metamaterials. In 2017, he enrolled in the Spanish National Research Council (CSIC) to conduct research on biomedical ultrasound applications at Instituto de Instrumentación para Imagen Molecular (i3M), UPV. He has been a Visiting Researcher at Columbia University, New York, NY, USA, and at the University of Salford, Manchester, U.K. Since 2013, he has authored or coauthored 29 journal papers and participated in more than 100 conferences. His research interests range from fundamental research in waves in complex and structured media to biomedical ultrasound applications.



Rubén Picó received the Ph.D. degree in physics from the Universitat Politècnica de València (UPV), València, Spain, and the Université du Maine, Le Mans, France, in 2004.

He was a Permanent Researcher and the Leader of the Acoustics Group in Complex Media, Instituto de Investigación para la Gestión Integrada de Zonas Costeras, UPV. He has participated in 20 research and development projects of national and international scope and leads as principal investigator six of them, among which two projects are included with the European Space Agency. He has supervised three doctoral theses and four on-going doctoral theses. He has authored or coauthored more than 40 scientific works in high impact journals and has participated in more than 100 national and international congresses.

Dr. Picó has been a member of the Technical committee of Ultrasound European Association since 2018. He is a reviewer of ten *Journal Citation Reports* in acoustics, ultrasound, and vibrations.



Joan Faus received the Ph.D. degree in odontology from the Universitat de Valéncia, Valéncia, Spain, in 2008.

He was an Associate Professor at the Universidad CEU Cardenal Herrera, Valéncia, Spain, between 2004 and 2012. He is the Founder and the Director of Instituto Valenciano de Investigaciones Odontológicas (IVIO), which is dedicated to teaching, research, and treatment in odontology. He is the Director of the IVIO Master in Periodontics and Osseointegration.

Dr. Faus is a member of the Sociedad Española de Periodoncia (SEPA), the Sociedad Española de Laser Odontologico (SELO), the International Team for Implantology (ITI), and the International Federation of dental educators and associations (IFDEA). He is the impeller of the IVIO-UPV Chair, which develops research and promotes odontology technology. He is the Co-Founder and a Coordinator of the surgery area V-BOPT in the Vertical Implantology Group.



Francisco Camarena received the Ph.D. degree in physics from the Universidad de València, València, Spain, in 2003.

He was a Founder Member and is the Head of the team Ultrasound Medical and Industrial Laboratory (UMIL) in 2009, which has formed part of the i3M since 2016. He was a Permanent Researcher at Instituto de Instrumentación para Imagen Molecular (i3M), Consejo Superior de Investigaciones Científicas (CSIC)-Universitat Politècnica de València (UPV), València, and a Professor with the Department of Applied Physics, UPV, València. He has participated in more than 80 national and international conferences related to acoustics and ultrasonics. He has authored or coauthored around 90 articles in national and international peer-reviewed journals.

Dr. Camarena is the Head of the Chair (Instituto Valenciano de Investigaciones Odontológicas) IVIO-UPV, dedicated to the promotion and development of training activities, research, dissemination, and technology transfer in the field of odontology. He is the Director of the Scientific Unit of Business Innovation (UCIE, i3M).